CHARACTERIZATION OF THE TRANSMIT POWER AND ANTENNA PATTERN OF THE GPS CONSTELLATION FOR THE CYGNSS MISSION

Tianlin Wang[1], Christopher Ruf[1,2], Bruce Block[3], Darren McKague[2]

[1]Department of Electrical Engineering and Computer Science
[2]Department of Climate and Space Sciences and Engineering
[3]Space Physics Research Laboratory
University of Michigan, Ann Arbor, MI USA

ABSTRACT

The Equivalent Isotropically Radiated Power (EIRP) by GPS satellites is needed to accurately calibrate the normalized bistatic radar cross section (NBRCS) measured by the Cyclone Global Navigation Satellite System (CYGNSS). EIRP is the product of GPS transmit power and antenna gain. To determine EIRP, we first estimate the GPS transmit power. A ground-based GPS constellation power monitor (GCPM) system has been built and calibrated to precisely measure GPS signals. The received power is repeatable and verified with German Aerospace Center (DLR)'s independent measurements. The estimated GPS transmit powers are validated with DLR's results and successfully applied to CYGNSS L1 calibration. GCPM measurements also demonstrate GPS antenna pattern asymmetries. Full GPS antenna patterns (over their terrestrial service volume) are estimated using the measurements made with the CYGNSS zenith antennas. CYGNSS zenith antenna measurements are able to sample the full transmit antenna pattern within a very short time.

***Index Terms*—** CYGNSS L1B calibration/validation, GPS EIRP, GPS constellation power monitor (GCPM), CYGNSS zenith antenna

1. INTRODUCTION

The Cyclone Global Navigation Satellite System (CYGNSS) is a space-borne mission to measure the ocean surface wind speed, including wind speeds in the inner core of tropical cyclones [1]. It uses a bi-static radar configuration, with the Global Positioning System (GPS) constellation (32 satellites) as the active source and the 8 CYGNSS micro-satellites as the passive receiver. CYGNSS Level 1 (L1) calibration/ validation includes: (1) L1A algorithm converts the Delay Doppler Maps (DDMs) to received power in watts, and (2) L1B algorithm computes the normalized bistatic radar cross section (NBRCS) from the received power and the external metadata [2]. The key part of the external metadata is the GPS Equivalent Isotropically Radiated Power (EIRP). GPS EIRP is a product of the transmit power and the transmit antenna gain, and determines the power incident on the ocean surface. Therefore, the accuracy and precision of the GPS EIRP are significant to the L1B calibration and to the accuracy of the Level 2 ocean surface wind speed and mean square slope (MSS) determination.

The GPS constellation has 3 different block types of space vehicle (SV) (12 IIR, 8 IIR-M and 12 IIF), with first 8 IIR SVs using the legacy antenna panel and all others using the improved antenna panel [3]. An estimation of GPS EIRP contains three main error sources: 1) unknown transmit powers of 32 GPS satellites (~4 dB variations among different GPS transmitters), 2) limited knowledge of the transmit antenna pattern (the patterns of 12 IIF SVs have not been released), 3) antenna gain uncertainty due to the azimuthal pattern asymmetry and the spacecraft yaw attitude maneuver [3, 4].

There are many challenges and difficulties in resolving the uncertainties: 1) expense and time required to use traditional high gain antenna dishes to measure the GPS received power, 2) no high quality absolute power calibration available for commercial GPS receivers, 3) with limited ground stations, it is not possible to retrieve the full transmit antenna pattern of all 32 GPS satellites.

In this paper, we present our progress in the GPS EIRP determination for CYGNSS L1B calibration. We have designed, implemented, and calibrated a ground-based GPS constellation power monitor (GCPM) system to measure the direct GPS signal [4]. Radiometric calibration and single PRN (pseudo random number) calibration are performed to accurately convert the received signal counts into power in watts. Calibrated GCPM received power is used to determine the GPS transmit power. We also demonstrate that the zenith antennas on the 8 CYGNSS microsatellites are able to provide full coverage of the GPS transmit antenna pattern (over the terrestrial service volume) with high revisit rates. Using calibrated CYGNSS zenith measurements, the retrieved antenna patterns of the entire GPS constellation can be determined, which will improve the accuracy of the CYGNSS L1B data products.

2. METHODOLOGY

DOI:10.1109/IGARSS.2018.8518531

The EIRP is the product of the transmit power P_T and antenna gain G_T of the GPS satellites. To retrieve the EIRP, the forward model is based on the Friis radar equation [5]:

$$P_R = \frac{[P_T G_T(\theta_T, \phi_T)]}{4\pi R^2 L_a}\left(\frac{\lambda^2}{4\pi}\right) G_R(\theta_R, \phi_R) \qquad (1)$$

where P_R is the received power of the direct GPS signal, G_R is the gain of receive antennas, R is the distance between the transmitter and the receiver, L_a is the atmospheric loss, λ is the wavelength for GPS L1 C/A signals, θ_T, θ_R are the off-boresight angles, and ϕ_T, ϕ_R are the around-boresight angles.

Eq. (1) is applicable to both measurements of direct GPS signals by the GCPM and the CYGNSS zenith antenna. The key term is the received power P_R, since all other components can be obtained from GPS receiver or estimated by a theoretical model. With a calibrated P_R, we are able to account for the time dependence of all variables due to the measurement geometry, and to estimate the EIRP.

The primary goal is to determine the GPS transmit power. We define a cost function computed from the GCPM measured received power and the forward model simulation (using the baseline antenna pattern in [3]). By minimizing the cost function, we can optimally search and determine the GPS transmit power for all 32 GPS satellites.

The secondary goal is to retrieve the transmit antenna pattern. The GCPM system provides accurate measurement of EIRPs. However, due to the limitation of observations by a single ground station, the full antenna pattern cannot be determined. We take advantage of the high revisit rate of CYGNSS satellites, and show that it provides full coverage of the transmit antenna pattern for the terrestrial service volume. We use the calibrated zenith measurements to retrieve the full antenna patterns for the entire constellation.

3. GPS CONSTELLATION POWER MONITOR

3.1. Design and Implementation

The GCPM system was designed and built at the Space Physics Research Laboratory and is mounted on the rooftop of the Space Research Building, University of Michigan, Ann Arbor [4]. As shown in Fig. 1, the GCPM system includes:

1). Outdoor: a passive Javad choke ring antenna (RHCP) is used to receive the direct GPS signal, and a thermally controlled, box-enclosed plate containing cold load, ambient load, excess noise source, and low noise amplifier (LNA) are used for stable signal amplification and calibration. The set point of a proportional–integral–derivative (PID) temperature controller, which controls the plate temperature, is 50 °C to ensure stable LNA gain and system noise figure for all ambient temperatures.

2). Indoor: a commercial Septentrio PolaRxS GPS receiver is used to measure the raw counts (proportional to GPS carrier power) of the GPS signals. The PC stores the raw data, controls the states of the calibration loads, and measures the temperature of the thermal control box.

More technical details of the GCPM system are in [4].

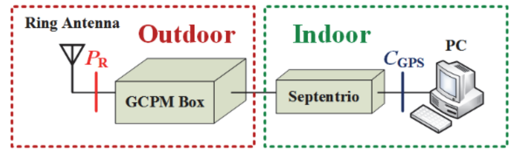

Fig. 1. The measurement setup of the GCPM system

3.2 Calibration

The main challenges of using a commercial GPS receiver are: 1) it only measures power in raw counts C_{GPS}, and there is no absolute power calibration to compute the received power P_R in watts; 2) it has a limited dynamic range.

Radiometric calibration using liquid nitrogen is performed to determine the system dynamic range [4]. The noise temperatures of the internal cold load, ambient load, and excess noise source are determined. Finally, the gain of the Septentrio receiver is set to a fixed 38 dB.

A single-PRN calibration using a CYGNSS GPS signal simulator (GSS) is performed. Fig. 2 shows the test configuration. The output power of the signal generator P_{SG} is measured by a calibrated power meter and is used to compute the power of reference signal P_{GSS} at the input port of the GCPM box. Combined with the measured counts C_{GSS}, we can compute a calibration scale factor, S_G, as

$$S_G = \frac{P_{GSS}}{C_{GSS}} = 6.10 \times 10^{-21}\ W/CT \qquad (2)$$

Note that this scaling factor is only applicable to this specific configuration of circuit elements and the current settings of system temperature and receiver gain. The received power is then calibrated using

$$P_R = S_G C_{GPS} \qquad (3)$$

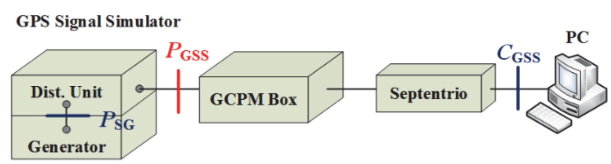

Fig. 2. Single PRN calibration using GSS

3.3 Stability of System Temperature Control

Three thermistor sensors measure the temperatures of the ambient load, the thermal plate, and the base plate in the GCPM box. Fig. 3 shows the long-term measurements over 50 days starting from February 2nd, 2018 with a 10 minutes sampling increment.

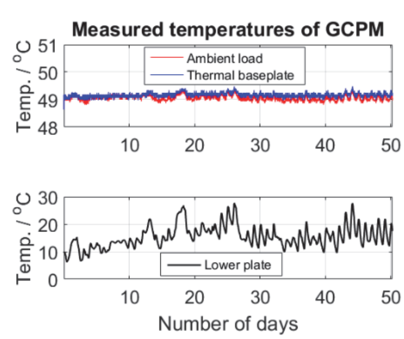

Fig. 3. Measured GCPM temperatures

The temperature of the base plate (no thermal control) shows the ambient diurnal variation. In contrast, the temperature of the ambient load (located on the thermal plate) has a mean value 49.06 ℃ with standard deviation 0.09 ℃; the temperature of the thermal plate has a mean value 49.17 ℃ with standard deviation 0.08 ℃. The GCPM system clearly shows stable temperature control, maintaining a stable LNA gain and system noise figure.

3.4 Performance Verification

In Fig. 4, independent measurements on two consecutive days are plotted. The timelines are shifted by 4 mins to account for orbit precession time differences. A 60-second moving average is applied, and the received power is calibrated referenced to the RF input of the GCPM box. The measured power is very repeatable even with most of the fine structures. The received power reflects the characteristics of the published GPS transmit antenna pattern in [3]: for example, PRN 16 of the legacy panel has a dip in the middle, while PRN 7 of the improved antenna panel has an enhanced power.

The power measured by GCPM for GPS PRN 29 was verified with independent measurements by German Aerospace Center (DLR) / German Space Operations Center (GSOC) using a 30 m dish antenna with 50 dB L-band gain. They agree well within 0.5 dB error, and the difference may be caused by an antenna gain pattern asymmetry [6].

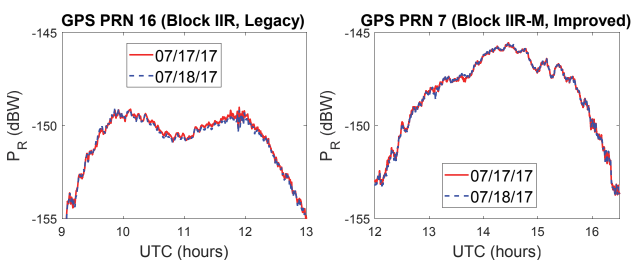

Fig. 4. Calibrated powers of GPS PRN 16 and PRN 7

4. SCIENCE RESULTS AND DISCOVERY

4.1 Estimation of GPS Transmit Power

Define a cost function as

$$\text{cost}(P_T) = \sum_{t=t_1}^{t_N} [P_R^{Model}(P_T, t) - P_R^{Meas}(t)]^2 \qquad (4)$$

where $P_R^{Model}(P_T, t)$ is the modeled received power using (1) with the baseline transmit antenna pattern in [3], $P_R^{Meas}(t)$ is the measured received power, and the summation is over the time from t_1 to t_N (effective measurement filtered by elevation mask = 20 degrees).

We search for an optimal solution for P_T by minimizing the cost function. By averaging 32 days of estimates of P_T, we determine the GPS transmit power (L1 C/A) for each satellite. Note that these solutions are the product of the

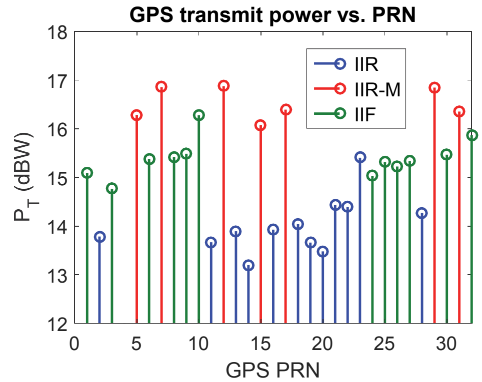

Fig. 5. Estimated GPS transmit power P_T vs. GPS PRN

transmit power and the gain correction factor (GCF). As shown in Fig. 5, the transmit power shows a block-type dependence, and the variation among different GPS transmitters is greater than 4 dB. The estimated GPS transmit power for the limited IIR-M block satellites is comparable to the previous values reported in [7, 8].

Fig. 6 compares the calibrated GPS EIRP (black curve, using calibrated transmit power P_T and baseline antenna pattern for G_T) and the measured EIRPs (red and blue curves computed directly from the GCPM received signal on July 30th and Oct 2nd, 2017, respectively). They agree well and demonstrate the effectiveness of the calibrated GPS transmit power. Note that the oscillations for off-boresight angles greater than 10 degrees may be caused by multipath effects.

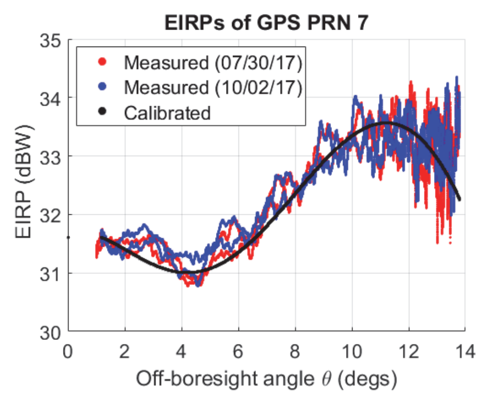

Fig. 6. Measured and calibrated EIRPs

The GPS transmit power has been applied to the CYGNSS L1 calibration for v2.0 data, and been shown by the CYGNSS Cal/Val team and Science team to have successfully reduced the PRN dependence of L1 NBRCS and L2 wind speed calibration.

4.2 Demonstration of Azimuthal Pattern Asymmetry

The left plot of Fig. 7 shows the relative cuts through the transmit antenna pattern of GPS PRN 5 on July 30th and Oct 2nd, 2017. There are two distinct branches in the 1st and 2nd quadrants, representing the antenna gains at different azimuth angles. In the right plot of Fig. 7, the two branches of the measured EIRPs separate with each other, which is a strong evidence of an antenna pattern azimuthal asymmetry. It demonstrates the necessity of including the azimuth dependence of antenna gain as well as the spacecraft yaw attitude [9] in the CYGNSS L1B algorithm.

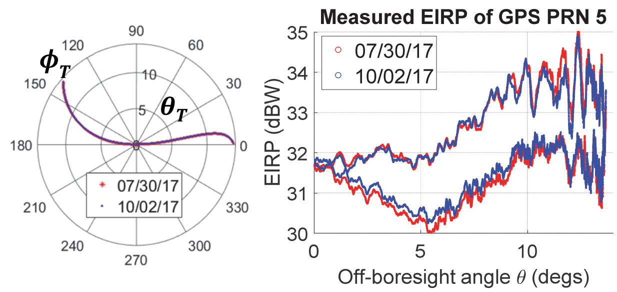

Fig. 7. Cuts through the pattern and GCPM's measured EIRPs

5. CYGNSS ZENITH ANTENNA MEASUREMENT

Because of the repeatability of GPS overpasses, ground station systems are unable to cover the full plane of transmit antenna pattern within a short time.

We take advantage of the wide coverage of the CYGNSS satellites and use their zenith antenna measurement of the GPS direct signal. Fig. 8 shows three weeks of pattern coverage for GPS PRN 1. The dense measurements over a relatively short time demonstrates that it is a viable technique to retrieve the full antenna pattern for the GPS terrestrial service volume (off-boresight angles $\theta_T <$ 13.8°, as the region bounded by the red circle).

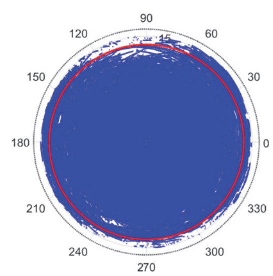

Fig. 8. Cuts through the pattern from CYGNSS

We are in the process of performing an absolute power calibration of the zenith antenna measurement using an engineering (Eng) model of the CYGNSS Delay-Doppler Mapping Receiver (DMR), as shown in Fig. 9. The DMR, zenith LNA and GSS are used to emulate the on-orbit zenith measurement.

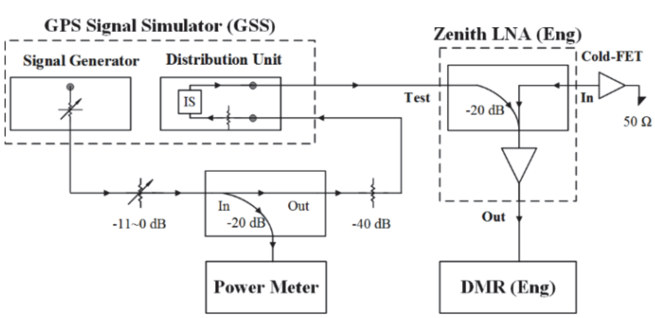

Fig. 9. Calibration scheme of CYGNSS zenith measurement

Testing of the DMR-GSS calibration and retrieval of the full antenna patterns are currently in progress; results will be reported in the conference presentation.

6. CONCLUSIONS AND FUTURE WORK

In this paper, we analyze the error sources for GPS EIRP and develop techniques to resolve the uncertainties in EIRP, including calibration of the absolute transmit power and transmit antenna gain pattern.

A GCPM system has been developed and calibrated to receive the direct GPS signal. The system temperature control is very stable and the received powers are highly repeatable. Results are verified by DLR's independent measurements. Advantages of the GCPM include: low cost, high robustness, and full constellation monitoring. The GPS transmit powers were calibrated and applied to the CYGNSS L1B algorithm. It successfully reduces the PRN dependence of CYGNSS L1 and L2 data products.

To retrieve the full pattern of GPS transmit antenna over the terrestrial service volume, the CYGNSS zenith antenna will be used. We have demonstrated the feasibility and are in process of calibration and validation of the zenith antenna measurement. The retrieved full antenna pattern of the entire GPS constellation will further improve the data quality and accuracy of CYGNSS L1B NBRCS.

7. REFERENCES

[1] C. S. Ruf, A. Lyons, M. Unwin, J. Dickinson, R. Rose, D. Rose, and M. Vincent, "CYGNSS: Enabling the Future of Hurricane Prediction," *IEEE Geoscience and Remote Sensing Magazine*, vol. 1, no. 2, pp. 52-67, June 2013.

[2] Ruf, C. S., et al, *CYGNSS Handbook*, Michigan Publishing, Ann Arbor, MI, 2016.

[3] W. A. Marquis and D. L. Reigh, "The GPS Block IIR and IIR-M Broadcast L-band Antenna Panel: Its Pattern and Performance," *Navigation*, vol. 62, no. 4, pp. 329-347, Dec. 2015.

[4] T. Wang, C. Ruf, S. Gleason, B. Block, D. McKague, and D. Provost, "Development of GPS Constellation Power Monitor System for High Accuracy Calibration/Validation of the CYGNSS L1B Data," *IGARSS*, pp. 1008-1011, July 2017.

[5] Ulaby, F. T., et al, *Microwave Radar and Radiometric Remote Sensing*, University of Michigan Press, Ann Arbor, MI, 2014.

[6] S. Thoelert, A. Hauschild, P. Steigenberger, and R. Langley, "GPS IIR-M L1 Transmit Power Redistribution: Analysis of GNSS Receiver and High-Gain Antenna Data," *Proc. 30th ION GNSS+*, pp. 1589-1602, Sept. 2017.

[7] A. Wu, "Predictions and Field Measurements of the GPS Block IIR L1 and L2 Ground Powers," *ION NTM*, pp. 931–938, Jan. 2002.

[8] P. Steigenberger, S. Thoelert, and O. Montenbruck, "GNSS Satellite Transmit Power and Its Impact on Orbit Determination," *Journal of Geodesy*, pp. 1-16, 2017.

[9] Y. E. Bar-Sever, "A New Model for GPS Yaw Attitude," *Journal of Geodesy,* vol. 70, no.11, pp. 714-723, 1996.